

## CYCLOTRON RESONANCE OF CURRENT CARRIERS IN ALUMINUM

R. T. MINA, V. S. ÉDEL'MAN, and M. S. KHAÏKIN

Institute of Physics Problems, Academy of Sciences, U.S.S.R.; Erevan Physics Institute

Submitted to JETP editor June 24, 1966

J. Exptl. Theoret. Phys. (U.S.S.R.) 51, 1363-1368 (November, 1966)

Cyclotron resonance of electrons and holes in the (010) aluminum plane is investigated at frequencies of 9.45 and 18.7 GHz. More exact values of the effective masses are obtained. The effective potential of the lattice,  $V_{002} = 0.068 \epsilon_F$ , is estimated on basis of the mass anisotropy of the holes of the central cross section. Cyclotron resonances occurring on non-central extreme cross sections of the hole surface, the existence of which does not follow from the 1-OPW model, are considered.

THE Fermi surface of aluminum was investigated recently by almost all presently known methods. The most information on the shape of the Fermi surface was obtained from measurements of the attenuation of ultrasound<sup>[1]</sup> and from a study of the quantum oscillations of the resistance.<sup>[2]</sup> The shape of the model of the Fermi surface, calculated in<sup>[3]</sup> in the approximation of four orthogonalized plane waves (4-OPW), is in detailed agreement with the experiments.<sup>[1,2]</sup> The results of an investigation of cyclotron resonance (c.r.) have shown that although the anisotropy of the effective masses is described satisfactorily by the 1-OPW model,<sup>[4]</sup> the values of the effective masses are  $\sim 1.5$  times larger than those calculated by the model. Such a discrepancy is connected with the fact that the velocities of the carrier are  $\sim 1.5$  times smaller than the velocity

$$v_c = p_c / m_e, \quad (1)$$

where  $p_c$  is the Fermi momentum. This circumstance makes a study of the carrier velocity more interesting, and especially investigations of c.r., which make it possible to measure accurately the carrier revolution periods.

The experiments described below were made with single-crystal aluminum, which was investigated by Vol'skiĭ.<sup>[2]</sup> The measurements were made only for the (010) crystallographic plane, since the corresponding results of Spong and Kip<sup>[5]</sup> are incomplete, and the accuracy of the measurements in the work of Galkin, Naberezhnykh, et al.<sup>[6,7]</sup> are lower by almost one order of magnitude.

## EXPERIMENT

The single crystal used for the present paper and in<sup>[2]</sup> was grown in a dismountable graphite

mold from molten aluminum with a residual resistance  $10^{-10}$  ohm-cm at 4.2° K. The sample was in the form of a disc 18 mm in diameter and 1.5 mm thick. The crystallographic plane (010) coincided with the flat surface of the disc with accuracy  $\sim 1^\circ$ . Etching in a boiling 20% aqueous solution of KOH for 15 minutes, removed from the surface of the sample a layer of metal 10-20  $\mu$  thick; the surface left by such a treatment was even and dull. The single crystal was placed in a strip resonator with linear polarization of the high frequency current. The investigations of the c.r. were made at two frequencies, 9.45 and 18.7 GHz, by the method of frequency modulation<sup>[8]</sup> in a magnetic field up to 10 kOe at a sample temperature 1.5° K. The cooling of the sample from 4.2 to 1.5° K more than doubled the c.r. amplitude.

Figure 1 shows an example of the c.r. A and  $\gamma$  with two greatly different periods. In our experiments we usually resolved the following c.r.:  $\gamma$ —up to order 4-6, A—up to order 10. According to Chambers,<sup>[9]</sup> the relative width of the c.r. line  $\delta H_n^{-1} / H_n^{-1} \approx (\omega\tau)^{-1}$ . Consequently, the electron mean free time at 1.5° K amounted in the investigated sample to  $(2-4) \times 10^{-10}$  sec, and the mean free path was 0.3-0.5 mm.

## EFFECTIVE MASSES OF ELECTRONS

The values of the effective masses were determined from spectra similar to those shown in Fig. 1, by the formula

$$\mu = m^* / m_e = e / m_e c \omega \Delta H^{-1}, \quad (2)$$

where  $\Delta H^{-1}$  is the c.r. period as a function of the reciprocal magnetic field  $H^{-1}$ . The results of the measurements for different directions of the field  $H$  in the (010) plane are shown in the diagrams of

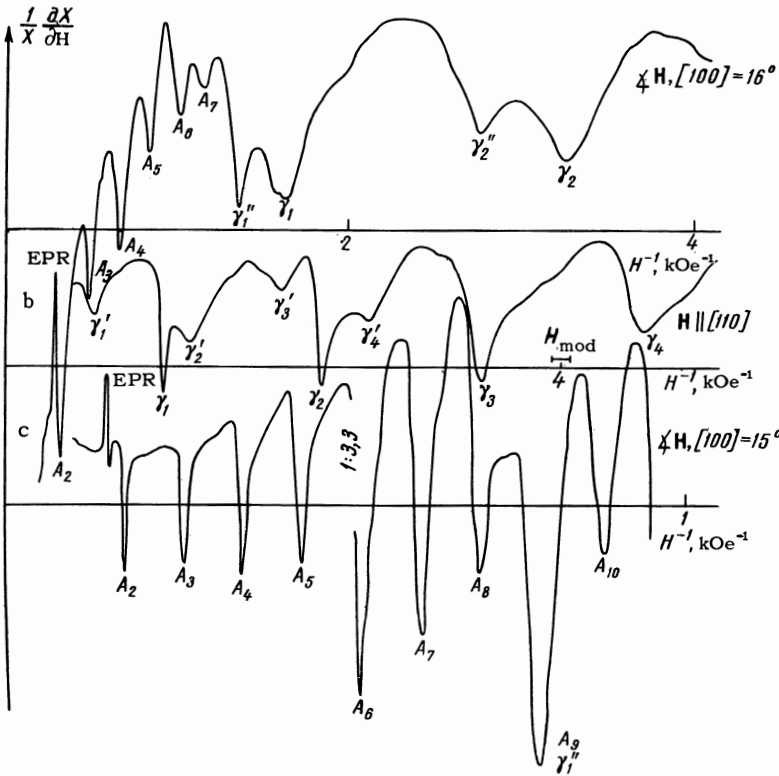


FIG. 1. Plots of the logarithmic derivative of the reactive part of the surface impedance of aluminum as a function of the reciprocal magnetic field. The letters A,  $\gamma$ ,  $\gamma'$  and  $\gamma''$  denote series of cyclotron resonances with different periods; the indices denote the order of the resonance. The orientation of the magnetic field in the crystallographic plane (010), which coincides with the surface of the sample, is indicated on the right side of the curves. The cyclotron resonance spectrum a was obtained at 9.45 GHz, and spectra b and c at 18.7 GHz. On curves a and c one sees the electron paramagnetic resonance (EPR). The left side of the spectrum b was recorded with a gain reduced by a factor 3.3. The section  $H_{mod}$  denotes the amplitude of the modulating field.

Fig. 2. In the right-hand diagram of this figure is shown the anisotropy of the effective masses corresponding to the c.r.  $\gamma$  of the electrons of the third zone. As shown in [2, 3] the electron Fermi surface of aluminum consists of tubes that narrow down on the ends, and whose axes have the {110} directions. This model is in good agreement with the results of the present work. Indeed, plots of the  $\gamma$  effective masses are linear in their central parts, and deviate noticeably from straight lines towards the smaller effective masses as the magnetic field is rotated. The latter circumstance is revealed immediately when the spectrum of Fig. 1b,

obtained for  $H \parallel [101]$  is examined. For cylindrical tubes, the period of the c.r.  $\gamma$  should be twice as large as the period of the c.r.  $\gamma'$  (Fig. 2). It is seen from Fig. 1b that this is not the case: the periods differ only by a factor  $\sim 1.8$  (see also Fig. 2,  $\gamma$  and  $\gamma'$  masses). Consequently, the tubes narrow down towards the ends. This fact was first established experimentally in a study of quantum oscillations of the surface resistance [2] and is confirmed by the results of the present investigation, in which the measurements were made in a much larger range of angles between  $H$  and [101].

Owing to the use of several c.r. periods for the

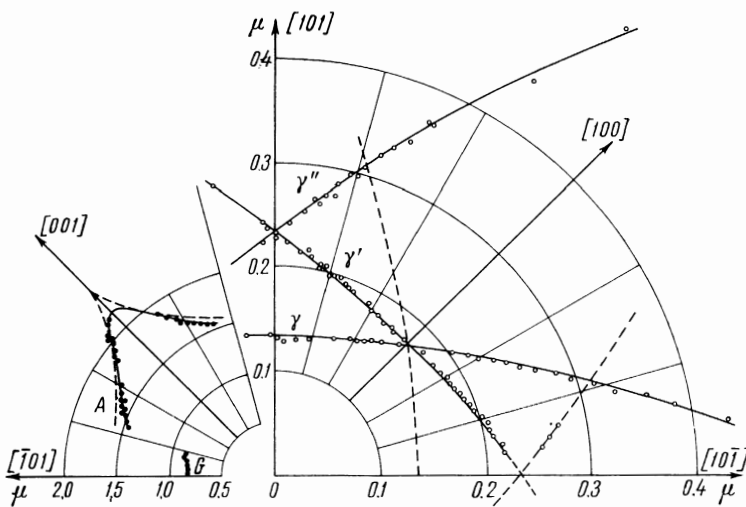


FIG. 2. Anisotropy of effective masses  $\mu$  of the carriers in aluminum in the (010) plane. On the left diagram, the dashed lines, show the anisotropy of the effective mass A, calculated by the 1-OPW model [5], in which we chose  $v_F = v_c / 1.6$ .

measurement of each value of the effective mass, the accuracy attained in the present work is almost one order of magnitude higher than that of Galkin et al.<sup>[6]</sup> For example, for  $\mathbf{H} \parallel [101]$  we obtained for the effective mass a value  $\mu = 0.132 \pm 0.001$ , whereas in <sup>[6]</sup> the corresponding mass is  $\mu = 0.4$ —a difference of 5%; when  $\mathbf{H} \parallel [100]$  this difference reaches 12%. In connection with the low accuracy of the measurements, the interpretation of the c.r.  $\kappa$  in <sup>[6]</sup> is apparently incorrect: within the limits of experimental error, the branch of the plot of the  $\kappa$  effective mass must be regarded as a continuation of the lines  $\gamma$  and  $\beta'$  (Fig. 5 in <sup>[4]</sup>), as should indeed be the case in accord with Fig. 2.

Larson and Gordon<sup>[10]</sup> determined the effective masses of the electrons from the temperature dependence of the oscillations of the de Haas–van Alphen effect. The table illustrates the good agreement between the mass values obtained in <sup>[10]</sup> and the present results.

$\angle \mathbf{H}, [100],$ deg	$\mu$			$\frac{\mu_{\text{exp}}}{\mu_{\text{theor}}}$
	de Haas–van Alphen ef- fect <sup>[10]</sup>	Cyclotron resonance	The- ory <sup>[2]</sup>	
0,1	$0.180 \pm 0.004$	$0.178 \pm 0.002$	0.136	1.31
5,0	$0.165 \pm 0.004$	$0.165 \pm 0.002$	—	—
25	$0.137 \pm 0.003$	$0.140 \pm 0.001$	—	—
25	$0.191 \pm 0.005$	$0.192 \pm 0.002$	—	—
40	$0.131 \pm 0.003$	$0.133 \pm 0.001$	—	—
44,9	$0.227 \pm 0.004$	$0.234 \pm 0.002$	—	—
45	$0.130 \pm 0.003$	$0.132 \pm 0.001$	0.095	1.39

## EFFECTIVE MASSES OF HOLES

In the left side of Fig. 2 is shown the anisotropy of the effective masses of the holes corresponding to c.r. A and G. The 1-OPW model<sup>[4]</sup> of the hole surface of the second zone is shown in Fig. 3. According to the results of a number of papers,<sup>[1, 5, 7, 11]</sup> in which different investigation methods were used, this model is quite close in shape to the true Fermi surface and differs from the latter only in slight rounding off of the edges. The agreement between the results of the experimental study of c.r. of the 1-OPW model was discussed in detail in the papers of Naberezhnykh and Tolstoluzhskii<sup>[7]</sup> and Spong and Kip,<sup>[5]</sup> and is confirmed in the present work. Indeed, the anisotropy of the mass A (Fig. 2) agrees satisfactorily with that calculated with the 1-OPW model.<sup>[7]</sup>

**Central hole orbit.** The effective mass A (Fig. 2) corresponds to the effective mass A of <sup>[7]</sup> and to the mass L of <sup>[5]</sup>. It is shown in these papers that the mass A pertains to the central section of the hole surface (Fig. 3). When the direction of the magnetic field coincides with a four fold axis (for example, [001]), the plane of the or-

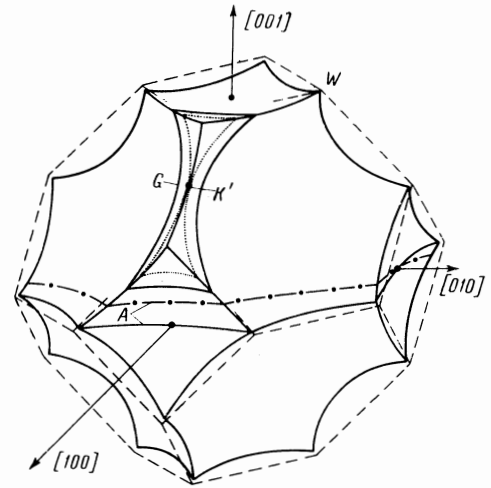


FIG. 3. Hole surface of aluminum in accordance with the 1-OPW model. The dashed line shows the Brillouin zone, part of which has been removed to simplify the figure. The line made up of points shows the orbit containing the singular point  $K'$ , while the solid line shows the following extremal orbits: non-central G at  $\mathbf{H} \parallel [101]$ , and two central ones A at  $\mathbf{H} \parallel [001]$  and  $\angle \mathbf{H}, [001] = \varphi \approx 5^\circ$ ; the latter is shown dash-dotted.

bit coincides with the Brillouin plane, and the orbit itself passes over the “ribs” of the hole surface. In this case the c.r. has low intensity and is not observed. As the field turns away from the [001] axis, the orbit moves away from the ribs of the surface, and the c.r. amplitude becomes noticeable. The c.r. corresponding to the central orbit on the hole surfaces of lead<sup>[12]</sup> and indium<sup>[13]</sup> behaves in perfect analogy; the only major difference is that the c.r. on lead and indium can be observed also when  $\mathbf{H} \parallel [001]$ .

As shown in <sup>[13]</sup>, the character of the deviation of the measured effective mass A from that calculated in the 1-OPW model makes it possible to estimate the Fourier component  $V_{002}$  of the effective potential of the lattice (Fig. 9b in <sup>[13]</sup>). Unfortunately, the mass A was not traced in aluminum continuously to  $\mathbf{H} \parallel [001]$ . However, as seen from Fig. 2, the experimental values of the A mass agree, within the limits of measurement accuracy, with the calculations for an angle  $2.5\text{--}3^\circ$  between  $\mathbf{H}$  and [001]. Consequently, at such directions of the field  $\mathbf{H}$  the hole orbit passes over sections of the Fermi surface which are not distorted by the influence of the potential  $V_{002}$ . On the basis of this we can estimate the maximum value of  $V_{002}$ , using formula (12) of <sup>[13]</sup>:

$$V_{002} \approx 2[(h/a)^2/2m][\sqrt{2} - (p_c^2(h/a)^2 - 1)^{1/2}]\varphi, \quad (3)$$

$$\varepsilon_F = p_c^2/2m,$$

where we put  $\varphi \leq 2.5\text{--}3^\circ$ . We obtain

$$\Gamma_{002}/\epsilon_F \approx (1.78/1.28)\varphi \leq 0.068 \pm 0.005. \quad (4)$$

This value of the effective potential is in good agreement with that obtained in the calculations of [3], namely  $V_{002} = 0.66 \epsilon_F$ .

Non-central hole orbit G. Figure 2 shows the effective mass G; no such mass is observed in [5], and in [7] it was observed, but its origin was not explained. Yet an interpretation of the cyclotron resonance G and of a few other resonances reported in [5] is worthy of attention.

Calculation of the effective masses of the holes by the 1-OPW model, which consists in simply summing the angular dimensions of the arcs making up the orbit, as a function of  $\rho_H$  (distance from the center of the zone to the plane of the orbit), gives a monotonic decrease of the mass (solid curve of Fig. 4) when  $\rho_H$  approaches the value at which the self-intersection point  $K'$  appears on the orbit (Fig. 3). If we recognize, however, that with this the section of the real hole Fermi surface approaches the hyperbolic limiting point, then it becomes obvious that the effective mass of the holes should increase without limit, as is shown qualitatively by the dashed curve of Fig. 4. This results in an extremal value of the mass G, to which one must indeed refer the cyclotron resonance observed at directions  $H$  close to the  $\{110\}$  axes.

The necessary correction of the results of the calculations by the 1-OPW model should be made also in plots of the masses E, F, and I of [5]. The orbits corresponding to them approach with increasing  $\rho_H$  different hyperbolic limiting points situated on the Fermi surface, as a result of which these three masses acquire extremal values. Thus, the cyclotron resonances E, F, and I should be assigned to non-central extremal sections of the hole surface. In this connection, the attempt made by Spong and Kip [5] to explain the possibility of cyclotron resonance on "almost extremal" orbits apparently becomes groundless.

In conclusion we note that the investigation reported in this paper has made it possible to measure the exact values of many effective masses of electrons and holes, determine the value of one component of the effective potential of the lattice, and explain the origin of a number of cyclotron resonances on non-central extremal sections of the hole surface.

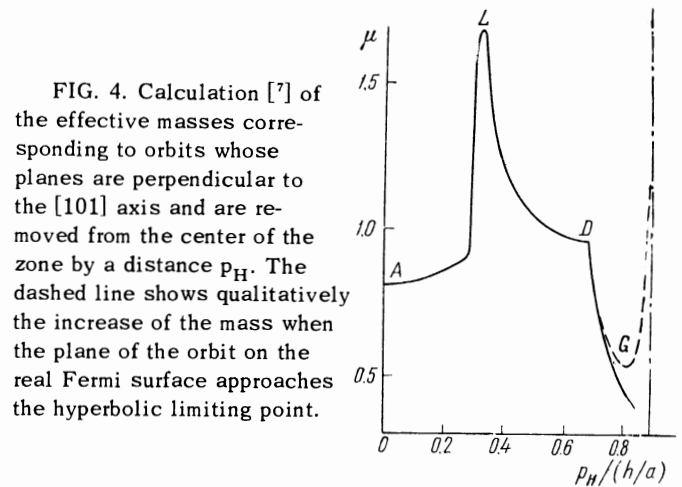


FIG. 4. Calculation [7] of the effective masses corresponding to orbits whose planes are perpendicular to the  $[101]$  axis and are removed from the center of the zone by a distance  $\rho_H$ . The dashed line shows qualitatively the increase of the mass when the plane of the orbit on the real Fermi surface approaches the hyperbolic limiting point.

The authors thank P. L. Kapitza for interest and attention to the work and G. S. Chernyshev and V. A. Yudin for technical help.

<sup>1</sup>G. N. Kamm and H. V. Bohm, *Phys. Rev.* **131**, 111 (1963).

<sup>2</sup>E. P. Vol'skiĭ, *JETP* **46**, 123 (1964), *Soviet Phys. JETP* **19**, 89 (1964).

<sup>3</sup>N. W. Ashcroft, *Phil. Mag.* **8**, 2055 (1963); W. A. Harrison, *Phys. Rev.* **118**, 1182 (1960).

<sup>4</sup>W. A. Harrison, *Phys. Rev.* **116**, 555 (1959).

<sup>5</sup>F. W. Spong and A. F. Kip, *Phys. Rev.* **137**, 431 (1965).

<sup>6</sup>A. A. Galkin, V. P. Naberezhnykh, and V. L. Mel'nik, *FTT* **5**, 201 (1963), *Soviet Phys. Solid State* **5**, 145 (1963).

<sup>7</sup>V. P. Naberezhnykh and V. P. Tolstoluzhskii, *JETP* **46**, 18 (1964), *Soviet Phys. JETP* **19**, 13 (1964).

<sup>8</sup>M. S. Khaĭkin, *PTÉ* No. 3, 95 (1961).

<sup>9</sup>R. G. Chambers, *Proc. Phys. Soc.* **86**, 305 (1965).

<sup>10</sup>C. O. Larson and W. L. Gordon, *Phys. Lett.* **15**, 121 (1965).

<sup>11</sup>M. G. Priestly, *Phil. Mag.* **7**, 1205 (1962).

<sup>12</sup>R. T. Mina and M. S. Khaĭkin, *JETP* **45**, 1304 (1963), *Soviet Phys. JETP* **18**, 896 (1964).

<sup>13</sup>R. T. Mina and M. S. Khaĭkin, *JETP* **51**, 62 (1966), *Soviet Phys. JETP* **24**, 42 (1967).

Translated by J. G. Adashko